

卒研配属学生向け
研究論文の読み方

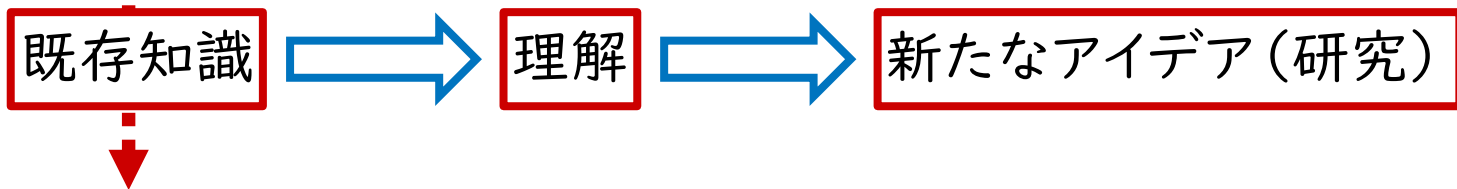
理学部 物理学科
固体物理学講座
西沢 グループ



なぜ論文を読むのか

最新の研究を行うには、

- 何が求められているのか、何をしりたいのか
 - どのようにすれば明らかになるか
 - どのように考えればいいのか
- が分かる必要がある



- これまでに何がわかっているか、何がわかっていないのか
- 先人はどのようにして明らかにしたか
- 先人はどのように考えたか

論文に書いてある

ゼロから新たなアイデアは生まれない。
なぜならアイデアとは既存知識の組み合わせであるから。

既存知識にとらわれない新たなアイデアというものは存在しない。
たとえあっても同じことを世界の誰かはすでに考え、試した上で失敗している。

アイザック・ニュートン

『私がかなたを見渡せたのだとしたら、それは巨人の肩の上に立っていたからです。』

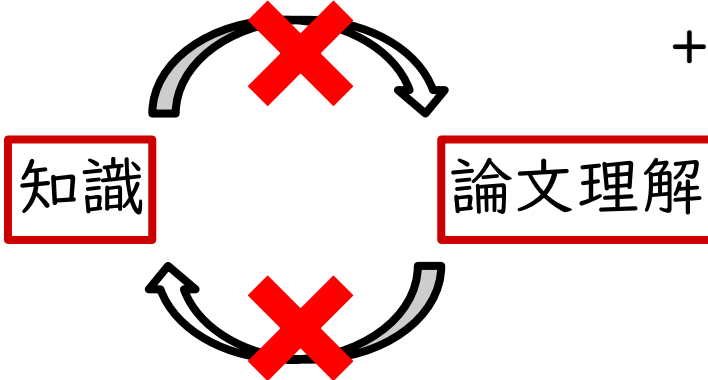
If I have seen further it is by standing on the shoulders of Giants.



学部生が論文を読む上での注意

知識が少ないから論文を理解できない

+ 英語が苦手で読むだけでも時間がかかる



論文が理解できないから知識が増えない

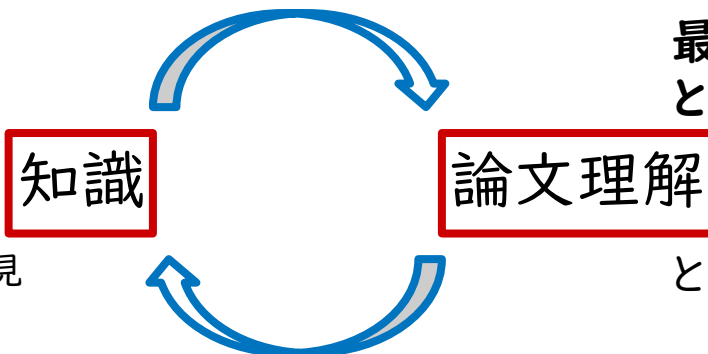
最初から全て理解しようとし
わからないところは放置か教員に聞く

少しでも知識があると理解できるところが増える

最初は日本語論文でもいいので、
とにかく理解のための前提知識を増やす



基礎物理
対象の性質
考え方
解析方法
得られた知見



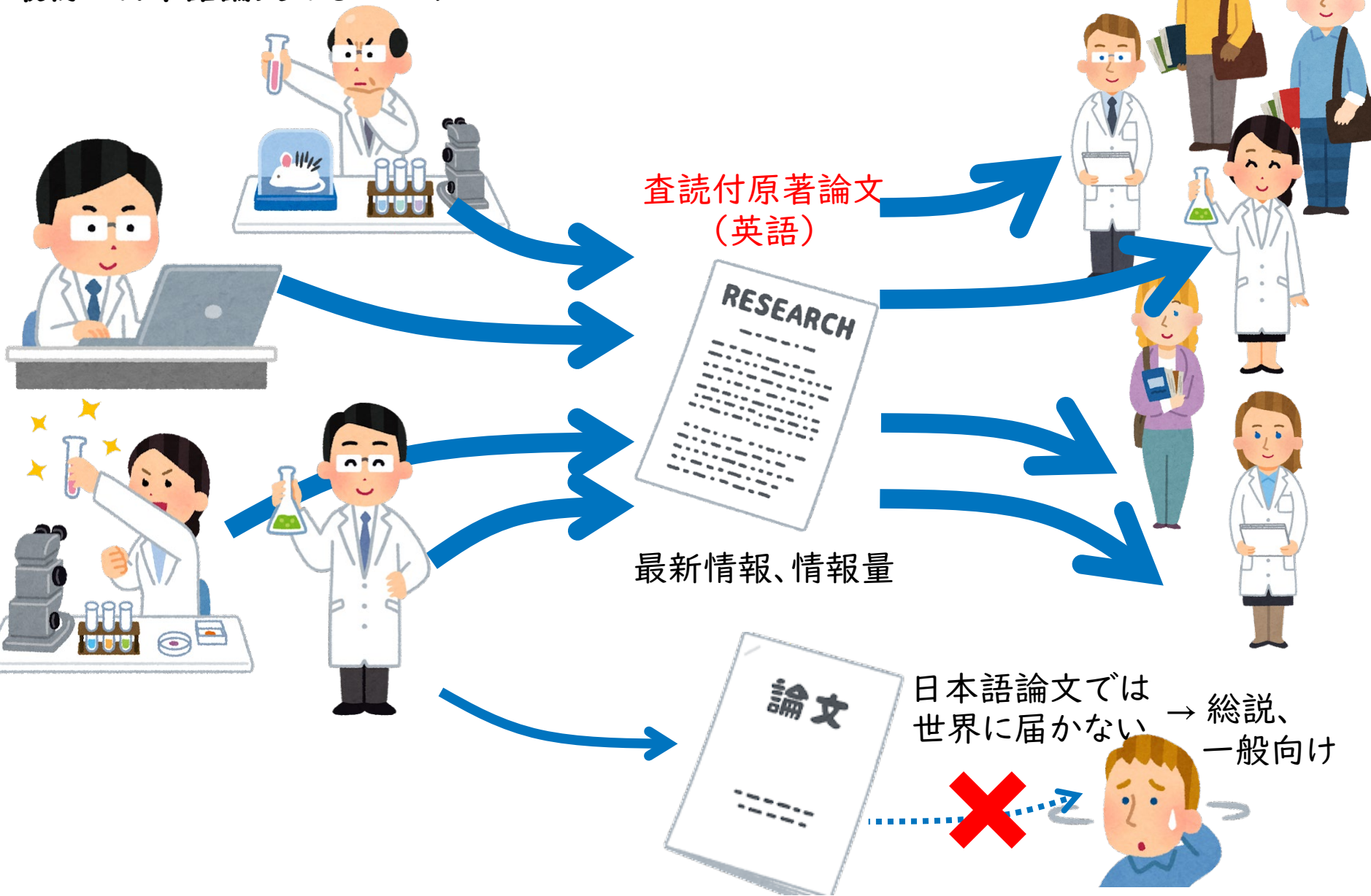
とにかくこのサイクルを回すことが大切



理解できる部分から分かる範囲のものを蓄積する

なぜ英語論文を読むべきなのか

最初は日本語論文でもいいけど……



査読付原著論文
(英語)



最新情報、情報量



日本語論文では世界に届かない → 総説、一般向け



配属学生向けの論文読みの進め方

1. 研究テーマに沿った日本語の総説を読む

知らない専門用語などは調べて
研究の流れ、必要な情報をざっくりと理解する

専門用語をざっくり掴むためには学部1~3年の授業が重要だったりする

このときに、キーワードとなる単語は英訳しておくこと



我々のグループの場合

- 日本レーザー医学会誌
2024年45巻 2号
- 「光アライアンス」2022年8月号
- 「光学」2023年5月号
(いずれも所属時に配布)

2. 研究テーマのうちで指標となっている英語原著論文のうちできるだけ最新のものを読む

研究の流れのうちでマイルストーンとなる論文は
必ず1.の日本語論文でも参照されているはず。
その論文(複数ある場合は最新のもの)を読む。
または配属された研究室(教授)が出した最新
の論文のうち最新かつ高IFのもの



- Kunnen *et al.*,
J. Biophotonics **8**, 317-323 (2015)
- N. Nishizawa *et al.*,
J. Biophotonics **14**, 202000380 (2020)

3. 2.を読んで理解を深める上で重要と思われる論文を過去に遡って読む もしくは、2.の論文を参照しているそれよりも新しい論文を読む

2.の論文を基点にして1つ**過去**のマイルストーン論文を読む
(1.の総説にも載っているはず)

同時に、2.の論文を基に研究された一つ**未来**の論文を読む



読む上でのポイント

1. 完璧を求めない

100%理解するなんて無理なので50%でOK、60%で上出来

2. 論文選びに迷ったら教員や先輩を頼る

最初は先人に貰うのが手っ取り早い

自分で選んでもこれでよさそうか聞こう

3. 最初から最後に向かってまっすぐ読まない

論文は小説ではないので最初から最後に向かって読む必要はない。

8ページ以降に示すような順序で読むと理解は早いと思われる

4. 論文の内容を鵜呑みしない

教科書ではないので、必ずしも正しいとは限らない

(そもそも大学以上では教科書も100%正しい訳では無いけど)

5. 論文の内容を自分の研究と結びつけておく

自分の研究と直接結びつかないと思われる論文であっても、

常に自分の研究との関連を意識しながら読む。

新たなアイデア(研究)になる可能性や自分の研究で予想外の結果が出たときの助けになることもあるが、それ以上に理解したことを記憶に定着させるのに役に立つ。

6. 英語翻訳ツールは使ってもいいが頼りすぎないこと

DeepLやGoogle翻訳などを使うことは悪いことではない。大枠を捉える、読むべきかどうかを判断するなどの場合は積極的に使う。ただし、本文を一度も読まずにコピペではいつまでたっても読めるようにはならない。辞書を使ってじっくり読む時間も作ること。

論文の読み方

1. 批判的に読む

常に疑問の姿勢で読む。良い論文の著者はその疑問を解消させるように書いている。
生じた疑問はメモをとっておき、それについて書いてあるかチェックする

2. 図(フローチャート)を書きながら読む

論理展開を→で結びながらフローチャートを書く。
論理の結びつき、対応、並列関係、因果関係を書く。

3. 紙に印刷し、色を付けながら読む

(私の場合)4色ボールペンを使う

Important sentence (重要な文章:赤だけ読んでも論文が一貫する文)

Unknown word (専門用語のうち知らない単語 → 後で復習)

Authors thoughts (著者の解釈、推測、結論)

My thoughts (3.の疑問、著者の考えに対する自分の意見)

4. 記録をつける

(私の場合)白紙の紙を用意して、そこに

フローチャート(4.)とともに**Important sentence** (3.の赤)、

著者の意見 (3.の青)、**自分で生じた疑問や意見** (5.の黒)

をまとめて書く。

それを論文の最後に入れてホッチキスでとめてファイリング

2番目に読む場所(図)の位置を把握する

次に読む(見る)のは、Figure Figureだけを抜き出して見てみる。

まずはCaptionと図を見て読み取れるかを眺めてみる。

縦軸や横軸、パラメータは理解できるものか

次に図とConclusionに短くまとめられていた結果と考察が結び付けられるかを見てみる

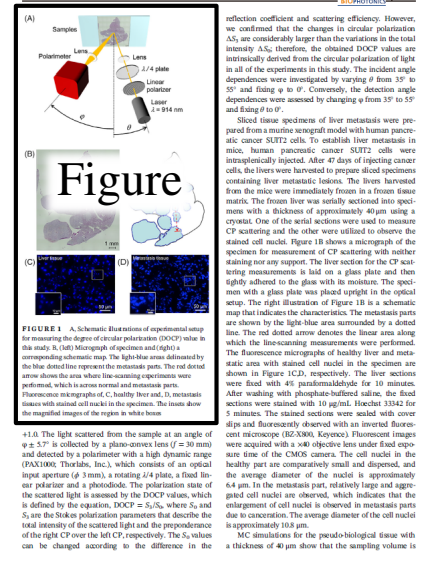
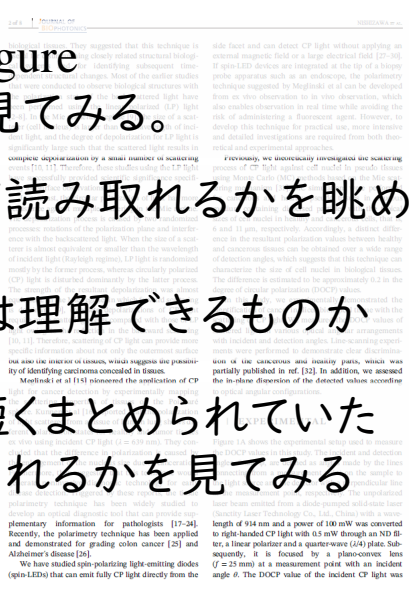
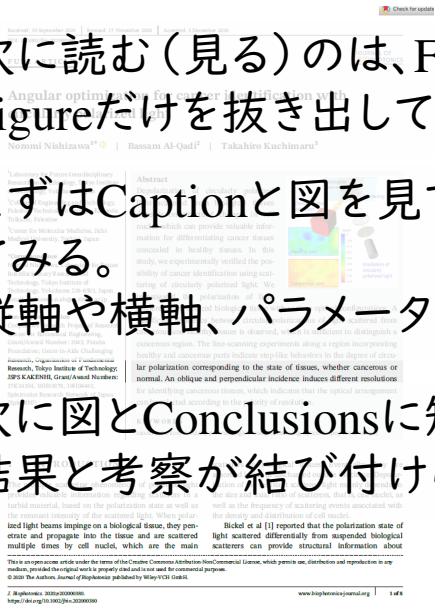


FIGURE 1 | A, Schematic illustration of experimental setup for measuring the degree of circular polarization (DOCP) values in the study. B, Color-micrograph of specimen and corresponding schematic map. The light-blue area delineated by the red circle line represents the irradiation part. The red dotted line indicates the scanning area. When the scanning experiments were performed, which is across normal and metastatic parts. Fluorescence micrograph of C, healthy liver and D, metastatic liver with stained cell nuclei in the specimen. The tissue shows the enlarged region of the region in white box.

reflection coefficient and scattering efficiency. However, the angular configurations. The sampling depth at $(\theta, \varphi) = (1^\circ, 30^\circ)$ is estimated to be 1.65 mm from the MC calculations for the tissue with infinite thickness [31]. Therefore, a significant portion of incident light is transmitted through the back of the sample or reflected at the interface between the specimen and the glass plate. The remaining portion of light and reflected light at the back undergo multiple scattering events in the entire sample with a thickness of 40 μm and then hit at the detector. This sampling volume includes approximately 750 nuclei on average.

3 | RESULTS AND DISCUSSION

Figure 2A,B shows the dependence of the DOCP value of scattered light on the incident angle θ and detection angle φ , respectively. The blue and red dots and lines represent the DOCP values measured at the point in the healthy and cancer (metastatic) parts, respectively. The DOCP values on the incident angle θ with $\varphi = 0^\circ$ shown in Figure 2A, indicates that the DOCP values from the healthy parts are larger than those from cancerous parts with an approximately constant difference of 0.20, except for the case with $\theta = 55^\circ$, where the DOCP values with increasing θ are different by approximately 0.20 between the DOCP values obtained from both parts. The former characteristics are due to the injection efficiency of CP light and irregular reduction at the Brewster angle when the incident angle approaches the interface angle between the air and the sample surface approximately 55° . In this study, the polarization component is dominantly penetrated into the sample, but the polarization component is mostly reflected because of the difference in reflectance at the surface [9]. Therefore, the CP of light penetrating into the tissue is decreased and the scattered light has less information inside the tissue. The result shows that almost zero DOCP values are observed at $(\theta, \varphi) = (55^\circ, 0^\circ)$. Moreover, the influence of surface reflection should be considered. Some of the incident CP light penetrates into tissues and provides information about the state of the sample. The remaining part of the incident light is irregularly reflected at the rough surface of the tissue. The sign of the DOCP of the reflected light is opposite to that of the incident CP light. As the incident direction approaches the detection direction, the component due to the irregular reflection in the total detected light becomes larger, resulting in a decrease (negative increase) in the DOCP value. When the difference between the incident and detection angles becomes less than 30° , most of the detected light is reflected light, which has insufficient information. The latter characteristic of the difference in the DOCP value corresponds reasonably well with the simulation results calculated for almost the same optical configurations (Figure 2C in ref. [31]), which implies that the observed difference in the DOCP value is derived from the difference in particle (cell nucleus) size. The magnification of the detected light becomes also influenced by extrinsic factors such as surface reflection, while the difference in the DOCP value is intrinsic and robust in the optical configuration with an angle within the appropriate range, which provides valuable information about the state of the biological tissue.

FIGURE 2 | Degree of circular polarization (DOCP) values as a function of A, incident angle θ with $\varphi = 0^\circ$ and, B, detection angle φ with $\theta = 0^\circ$, respectively.

is smaller than that from healthy tissues. However, this magnitude relation is opposite to the results shown in ref. [31], which are obtained using the incident CP light with $\lambda = 639 \text{ nm}$. Light scattering in the second radiation from the dipole excited by the first irradiation on the surface of the scatterer. The degree of depolarization varies according to the distribution of dipoles, and strongly depends on the ratio of the wavelength and size of the scatterer. We have calculated the wavelength dependence of the expected DOCP value of light scattered by noncancerous and cancerous pseudo-biological tissues in aqueous medium with dispersing scatterers having a diameter of 6.0 and 11.0 μm , respectively, by the same calculation method in ref. [31]. The calculated DOCP values show oscillating behavior derived from spherical harmonics with a variable size parameter, $x = ka$. The DOCP values from pseudo-cancerous tissue (P_{cancer}) are larger than those from pseudo-healthy tissue (P_{healthy}) at $\lambda = 639 \text{ nm}$, whereas $P_{\text{cancer}} < P_{\text{healthy}}$ at $\lambda > 639 \text{ nm}$. These calculation results can explain both experimental results.

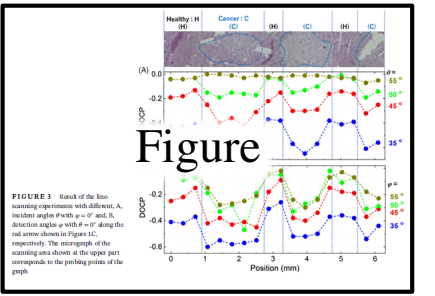


FIGURE 3 | Result of the line-scanning experiments with different A, incident angle θ with $\varphi = 0^\circ$ and, B, detection angle φ with $\theta = 0^\circ$ along the radial direction. The DOCP values from the healthy parts are larger than those from cancerous parts with an approximately constant difference of 0.20, except for the case with $\theta = 55^\circ$, where the DOCP values with increasing θ are different by approximately 0.20 between the DOCP values obtained from both parts.

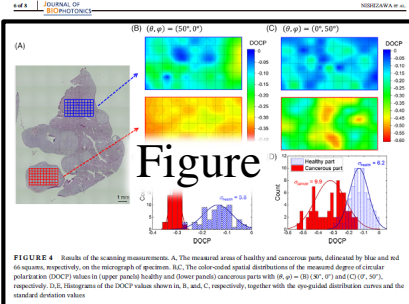


FIGURE 4 | Results of the scanning micrographs. A, The measured areas of healthy and cancerous parts, delineated by blue and red squares, respectively, on the micrograph of specimen. B, The color-coded spatial distributions of the measured degree of circular polarization (DOCP) values in (upper panel) healthy and (lower panel) cancerous parts with $(\theta, \varphi) = (0^\circ, 0^\circ)$ and $(0^\circ, 55^\circ)$, respectively. D, E, Histograms of the DOCP values shown in B, and C, respectively, together with the equalized distribution curves and the standard deviation values.

4 | CONCLUSION

We experimentally investigated the applicability of scattered CP light for cancer identification in optical

論理的にしっかりと結びつかなくともいいので、それぞれの図の論文中での位置づけを把握しておく。

この論文では、Figure 1は試料や実験方法について、Figure 2~4が実験結果で、それぞれ一点測定したもの、線上に測定したもの、面内を測定したもの、ぐらいが分かればいい。

[1] N. Nishizawa, B. Al-Qadiri, and T. Kuchimaru, "Angular optimization of circular polarization DOCP values for cancer identification," *Journal of Biophotonics*, vol. 14, no. 1, pp. 1-10, 2023. [2] N. Nishizawa, B. Al-Qadiri, and T. Kuchimaru, "Circular polarization DOCP values for cancer identification," *Journal of Biophotonics*, vol. 14, no. 1, pp. 1-10, 2023. [3] N. Nishizawa, B. Al-Qadiri, and T. Kuchimaru, "Circular polarization DOCP values for cancer identification," *Journal of Biophotonics*, vol. 14, no. 1, pp. 1-10, 2023. [4] N. Nishizawa, B. Al-Qadiri, and T. Kuchimaru, "Circular polarization DOCP values for cancer identification," *Journal of Biophotonics*, vol. 14, no. 1, pp. 1-10, 2023. [5] N. Nishizawa, B. Al-Qadiri, and T. Kuchimaru, "Circular polarization DOCP values for cancer identification," *Journal of Biophotonics*, vol. 14, no. 1, pp. 1-10, 2023. [6] N. Nishizawa, B. Al-Qadiri, and T. Kuchimaru, "Circular polarization DOCP values for cancer identification," *Journal of Biophotonics*, vol. 14, no. 1, pp. 1-10, 2023. [7] N. Nishizawa, B. Al-Qadiri, and T. Kuchimaru, "Circular polarization DOCP values for cancer identification," *Journal of Biophotonics*, vol. 14, no. 1, pp. 1-10, 2023. [8] N. Nishizawa, B. Al-Qadiri, and T. Kuchimaru, "Circular polarization DOCP values for cancer identification," *Journal of Biophotonics*, vol. 14, no. 1, pp. 1-10, 2023. [9] N. Nishizawa, B. Al-Qadiri, and T. Kuchimaru, "Circular polarization DOCP values for cancer identification," *Journal of Biophotonics*, vol. 14, no. 1, pp. 1-10, 2023. [10] N. Nishizawa, B. Al-Qadiri, and T. Kuchimaru, "Circular polarization DOCP values for cancer identification," *Journal of Biophotonics*, vol. 14, no. 1, pp. 1-10, 2023. [11] N. Nishizawa, B. Al-Qadiri, and T. Kuchimaru, "Circular polarization DOCP values for cancer identification," *Journal of Biophotonics*, vol. 14, no. 1, pp. 1-10, 2023. [12] N. Nishizawa, B. Al-Qadiri, and T. Kuchimaru, "Circular polarization DOCP values for cancer identification," *Journal of Biophotonics*, vol. 14, no. 1, pp. 1-10, 2023. [13] N. Nishizawa, B. Al-Qadiri, and T. Kuchimaru, "Circular polarization DOCP values for cancer identification," *Journal of Biophotonics*, vol. 14, no. 1, pp. 1-10, 2023. [14] N. Nishizawa, B. Al-Qadiri, and T. Kuchimaru, "Circular polarization DOCP values for cancer identification," *Journal of Biophotonics*, vol. 14, no. 1, pp. 1-10, 2023. [15] N. Nishizawa, B. Al-Qadiri, and T. Kuchimaru, "Circular polarization DOCP values for cancer identification," *Journal of Biophotonics*, vol. 14, no. 1, pp. 1-10, 2023. [16] N. Nishizawa, B. Al-Qadiri, and T. Kuchimaru, "Circular polarization DOCP values for cancer identification," *Journal of Biophotonics*, vol. 14, no. 1, pp. 1-10, 2023. [17] N. Nishizawa, B. Al-Qadiri, and T. Kuchimaru, "Circular polarization DOCP values for cancer identification," *Journal of Biophotonics*, vol. 14, no. 1, pp. 1-10, 2023. [18] N. Nishizawa, B. Al-Qadiri, and T. Kuchimaru, "Circular polarization DOCP values for cancer identification," *Journal of Biophotonics*, vol. 14, no. 1, pp. 1-10, 2023. [19] N. Nishizawa, B. Al-Qadiri, and T. Kuchimaru, "Circular polarization DOCP values for cancer identification," *Journal of Biophotonics*, vol. 14, no. 1, pp. 1-10, 2023. [20] N. Nishizawa, B. Al-Qadiri, and T. Kuchimaru, "Circular polarization DOCP values for cancer identification," *Journal of Biophotonics*, vol. 14, no. 1, pp. 1-10, 2023. [21] N. Nishizawa, B. Al-Qadiri, and T. Kuchimaru, "Circular polarization DOCP values for cancer identification," *Journal of Biophotonics*, vol. 14, no. 1, pp. 1-10, 2023. [22] N. Nishizawa, B. Al-Qadiri, and T. Kuchimaru, "Circular polarization DOCP values for cancer identification," *Journal of Biophotonics*, vol. 14, no. 1, pp. 1-10, 2023. [23] N. Nishizawa, B. Al-Qadiri, and T. Kuchimaru, "Circular polarization DOCP values for cancer identification," *Journal of Biophotonics*, vol. 14, no. 1, pp. 1-10, 2023. [24] N. Nishizawa, B. Al-Qadiri, and T. Kuchimaru, "Circular polarization DOCP values for cancer identification," *Journal of Biophotonics*, vol. 14, no. 1, pp. 1-10, 2023. [25] N. Nishizawa, B. Al-Qadiri, and T. Kuchimaru, "Circular polarization DOCP values for cancer identification," *Journal of Biophotonics*, vol. 14, no. 1, pp. 1-10, 2023. [26] N. Nishizawa, B. Al-Qadiri, and T. Kuchimaru, "Circular polarization DOCP values for cancer identification," *Journal of Biophotonics*, vol. 14, no. 1, pp. 1-10, 2023. [27] N. Nishizawa, B. Al-Qadiri, and T. Kuchimaru, "Circular polarization DOCP values for cancer identification," *Journal of Biophotonics*, vol. 14, no. 1, pp. 1-10, 2023. [28] N. Nishizawa, B. Al-Qadiri, and T. Kuchimaru, "Circular polarization DOCP values for cancer identification," *Journal of Biophotonics*, vol. 14, no. 1, pp. 1-10, 2023. [29] N. Nishizawa, B. Al-Qadiri, and T. Kuchimaru, "Circular polarization DOCP values for cancer identification," *Journal of Biophotonics*, vol. 14, no. 1, pp. 1-10, 2023. [30] N. Nishizawa, B. Al-Qadiri, and T. Kuchimaru, "Circular polarization DOCP values for cancer identification," *Journal of Biophotonics*, vol. 14, no. 1, pp. 1-10, 2023. [31] N. Nishizawa, B. Al-Qadiri, and T. Kuchimaru, "Circular polarization DOCP values for cancer identification," *Journal of Biophotonics*, vol. 14, no. 1, pp. 1-10, 2023. [32] N. Nishizawa, B. Al-Qadiri, and T. Kuchimaru, "Circular polarization DOCP values for cancer identification," *Journal of Biophotonics*, vol. 14, no. 1, pp. 1-10, 2023. [33] N. Nishizawa, B. Al-Qadiri, and T. Kuchimaru, "Circular polarization DOCP values for cancer identification," *Journal of Biophotonics*, vol. 14, no. 1, pp. 1-10, 2023. [34] N. Nishizawa, B. Al-Qadiri, and T. Kuchimaru, "Circular polarization DOCP values for cancer identification," *Journal of Biophotonics*, vol. 14, no. 1, pp. 1-10, 2023. [35] N. Nishizawa, B. Al-Qadiri, and T. Kuchimaru, "Circular polarization DOCP values for cancer identification," *Journal of Biophotonics*, vol. 14, no. 1, pp. 1-10, 2023. [36] N. Nishizawa, B. Al-Qadiri, and T. Kuchimaru, "Circular polarization DOCP values for cancer identification," *Journal of Biophotonics*, vol. 14, no. 1, pp. 1-10, 2023. [37] N. Nishizawa, B. Al-Qadiri, and T. Kuchimaru, "Circular polarization DOCP values for cancer identification," *Journal of Biophotonics*, vol. 14, no. 1, pp. 1-10, 2023. [38] N. Nishizawa, B. Al-Qadiri, and T. Kuchimaru, "Circular polarization DOCP values for cancer identification," *Journal of Biophotonics*, vol. 14, no. 1, pp. 1-10, 2023. [39] N. Nishizawa, B. Al-Qadiri, and T. Kuchimaru, "Circular polarization DOCP values for cancer identification," *Journal of Biophotonics*, vol. 14, no. 1, pp. 1-10, 2023. [40] N. Nishizawa, B. Al-Qadiri, and T. Kuchimaru, "Circular polarization DOCP values for cancer identification," *Journal of Biophotonics*, vol. 14, no. 1, pp. 1-10, 2023. [41] N. Nishizawa, B. Al-Qadiri, and T. Kuchimaru, "Circular polarization DOCP values for cancer identification," *Journal of Biophotonics*, vol. 14, no. 1, pp. 1-10, 2023. [42] N. Nishizawa, B. Al-Qadiri, and T. Kuchimaru, "Circular polarization DOCP values for cancer identification," *Journal of Biophotonics*, vol. 14, no. 1, pp. 1-10, 2023. [43] N. Nishizawa, B. Al-Qadiri, and T. Kuchimaru, "Circular polarization DOCP values for cancer identification," *Journal of Biophotonics*, vol. 14, no. 1, pp. 1-10, 2023. [44] N. Nishizawa, B. Al-Qadiri, and T. Kuchimaru, "Circular polarization DOCP values for cancer identification," *Journal of Biophotonics*, vol. 14, no. 1, pp. 1-10, 2023. [45] N. Nishizawa, B. Al-Qadiri, and T. Kuchimaru, "Circular polarization DOCP values for cancer identification," *Journal of Biophotonics*, vol. 14, no. 1, pp. 1-10, 2023. [46] N. Nishizawa, B. Al-Qadiri, and T. Kuchimaru, "Circular polarization DOCP values for cancer identification," *Journal of Biophotonics*, vol. 14, no. 1, pp. 1-10, 2023. [47] N. Nishizawa, B. Al-Qadiri, and T. Kuchimaru, "Circular polarization DOCP values for cancer identification," *Journal of Biophotonics*, vol. 14, no. 1, pp. 1-10, 2023. [48] N. Nishizawa, B. Al-Qadiri, and T. Kuchimaru, "Circular polarization DOCP values for cancer identification," *Journal of Biophotonics*, vol. 14, no. 1, pp. 1-10, 2023. [49] N. Nishizawa, B. Al-Qadiri, and T. Kuchimaru, "Circular polarization DOCP values for cancer identification," *Journal of Biophotonics*, vol. 14, no. 1, pp. 1-10, 2023. [50] N. Nishizawa, B. Al-Qadiri, and T. Kuchimaru, "Circular polarization DOCP values for cancer identification," *Journal of Biophotonics*, vol. 14, no. 1, pp. 1-10, 2023. [51] N. Nishizawa, B. Al-Qadiri, and T. Kuchimaru, "Circular polarization DOCP values for cancer identification," *Journal of Biophotonics*, vol. 14, no. 1, pp. 1-10, 2023. [52] N. Nishizawa, B. Al-Qadiri, and T. Kuchimaru, "Circular polarization DOCP values for cancer identification," *Journal of Biophotonics*, vol. 14, no. 1, pp. 1-10, 2023. [53] N. Nishizawa, B. Al-Qadiri, and T. Kuchimaru, "Circular polarization DOCP values for cancer identification," *Journal of Biophotonics*, vol. 14, no. 1, pp. 1-10, 2023. [54] N. Nishizawa, B. Al-Qadiri, and T. Kuchimaru, "Circular polarization DOCP values for cancer identification," *Journal of Biophotonics*, vol. 14, no. 1, pp. 1-10, 2023. [55] N. Nishizawa, B. Al-Qadiri, and T. Kuchimaru, "Circular polarization DOCP values for cancer identification," *Journal of Biophotonics*, vol. 14, no. 1, pp. 1-10, 2023. [56] N. Nishizawa, B. Al-Qadiri, and T. Kuchimaru, "Circular polarization DOCP values for cancer identification," *Journal of Biophotonics*, vol. 14, no. 1, pp. 1-10, 2023. [57] N. Nishizawa, B. Al-Qadiri, and T. Kuchimaru, "Circular polarization DOCP values for cancer identification," *Journal of Biophotonics*, vol. 14, no. 1, pp. 1-10, 2023. [58] N. Nishizawa, B. Al-Qadiri, and T. Kuchimaru, "Circular polarization DOCP values for cancer identification," *Journal of Biophotonics*, vol. 14, no. 1, pp. 1-10, 2023. [59] N. Nishizawa, B. Al-Qadiri, and T. Kuchimaru, "Circular polarization DOCP values for cancer identification," *Journal of Biophotonics*, vol. 14, no. 1, pp. 1-10, 2023. [60] N. Nishizawa, B. Al-Qadiri, and T. Kuchimaru, "Circular polarization DOCP values for cancer identification," *Journal of Biophotonics*, vol. 14, no. 1, pp. 1-10, 2023. [61] N. Nishizawa, B. Al-Qadiri, and T. Kuchimaru, "Circular polarization DOCP values for cancer identification," *Journal of Biophotonics*, vol. 14, no. 1, pp. 1-10, 2023. [62] N. Nishizawa, B. Al-Qadiri, and T. Kuchimaru, "Circular polarization DOCP values for cancer identification," *Journal of Biophotonics*, vol. 14, no. 1, pp. 1-10, 2023. [63] N. Nishizawa, B. Al-Qadiri, and T. Kuchimaru, "Circular polarization DOCP values for cancer identification," *Journal of Biophotonics*, vol. 14, no. 1, pp. 1-10, 2023. [64] N. Nishizawa, B. Al-Qadiri, and T. Kuchimaru, "Circular polarization DOCP values for cancer identification," *Journal of Biophotonics*, vol. 14, no. 1, pp. 1-10, 2023. [65] N. Nishizawa, B. Al-Qadiri, and T. Kuchimaru, "Circular polarization DOCP values for cancer identification," *Journal of Biophotonics*, vol. 14, no. 1, pp. 1-10, 2023. [66] N. Nishizawa, B. Al-Qadiri, and T. Kuchimaru, "Circular polarization DOCP values for cancer identification," *Journal of Biophotonics*, vol. 14, no. 1, pp. 1-10, 2023. [67] N. Nishizawa, B. Al-Qadiri, and T. Kuchimaru, "Circular polarization DOCP values for cancer identification," *Journal of Biophotonics*, vol. 14, no. 1, pp. 1-10, 2023. [68] N. Nishizawa, B. Al-Qadiri, and T. Kuchimaru, "Circular polarization DOCP values for cancer identification," *Journal of Biophotonics*, vol. 14, no. 1, pp. 1-10, 2023. [69] N. Nishizawa, B. Al-Qadiri, and T. Kuchimaru, "Circular polarization DOCP values for cancer identification," *Journal of Biophotonics*, vol. 14, no. 1, pp. 1-10, 2023. [70] N. Nishizawa, B. Al-Qadiri, and T. Kuchimaru, "Circular polarization DOCP values for cancer identification," *Journal of Biophotonics*, vol. 14, no. 1, pp. 1-10, 2023. [71] N. Nishizawa, B. Al-Qadiri, and T. Kuchimaru, "Circular polarization DOCP values for cancer identification," *Journal of Biophotonics*, vol. 14, no. 1, pp. 1-10, 2023. [72] N. Nishizawa, B. Al-Qadiri, and T. Kuchimaru, "Circular polarization DOCP values for cancer identification," *Journal of Biophotonics*, vol. 14, no. 1, pp. 1-10, 2023. [73] N. Nishizawa, B. Al-Qadiri, and T. Kuchimaru, "Circular polarization DOCP values for cancer identification," *Journal of Biophotonics*, vol. 14, no. 1, pp. 1-10, 2023. [74] N. Nishizawa, B. Al-Qadiri, and T. Kuchimaru, "Circular polarization DOCP values for cancer identification," *Journal of Biophotonics*, vol. 14, no. 1, pp. 1-10, 2023. [75] N. Nishizawa, B. Al-Qadiri, and T. Kuchimaru, "Circular polarization DOCP values for cancer identification," *Journal of Biophotonics*, vol. 14, no. 1, pp. 1-10, 2023. [76] N. Nishizawa, B. Al-Qadiri, and T. Kuchimaru, "Circular polarization DOCP values for cancer identification," *Journal of Biophotonics*, vol. 14, no. 1, pp. 1-10, 2023. [77] N. Nishizawa, B. Al-Qadiri, and T. Kuchimaru, "Circular polarization DOCP values for cancer identification," *Journal of Biophotonics*, vol. 14, no. 1, pp. 1-10, 2023. [78] N. Nishizawa, B. Al-Qadiri, and T. Kuchimaru, "Circular polarization DOCP values for cancer identification," *Journal of Biophotonics*, vol. 14, no. 1, pp. 1-10, 2023. [79] N. Nishizawa, B. Al-Qadiri, and T. Kuchimaru, "Circular polarization DOCP values for cancer identification," *Journal of Biophotonics*, vol. 14, no. 1, pp. 1-10, 2023. [80] N. Nishizawa, B. Al-Qadiri, and T. Kuchimaru, "Circular polarization DOCP values for cancer identification," *Journal of Biophotonics*, vol. 14, no. 1, pp. 1-10, 2023. [81] N. Nishizawa, B. Al-Qadiri, and T. Kuchimaru, "Circular polarization DOCP values for cancer identification," *Journal of Biophotonics*, vol. 14, no. 1, pp. 1-10, 2023. [82] N. Nishizawa, B. Al-Qadiri, and T. Kuchimaru, "Circular polarization DOCP values for cancer identification," *Journal of Biophotonics*, vol. 14, no. 1, pp. 1-10, 2023. [83] N. Nishizawa, B. Al-Qadiri, and T. Kuchimaru, "Circular polarization DOCP values for cancer identification," *Journal of Biophotonics*, vol. 14, no. 1, pp. 1-10, 2023. [84] N. Nishizawa, B. Al-Qadiri, and T. Kuchimaru, "Circular polarization DOCP values for cancer identification," *Journal of Biophotonics*, vol. 14, no. 1, pp. 1-10, 2023. [85] N. Nishizawa, B. Al-Qadiri, and T. Kuchimaru, "Circular polarization DOCP values for cancer identification," *Journal of Biophotonics*, vol. 14, no. 1, pp. 1-10, 2023. [86] N. Nishizawa, B. Al-Qadiri, and T. Kuchimaru, "Circular polarization DOCP values for cancer identification," *Journal of Biophotonics*, vol. 14, no. 1, pp. 1-10, 2023. [87] N. Nishizawa, B. Al-Qadiri, and T. Kuchimaru, "Circular polarization DOCP values for cancer identification," *Journal of Biophotonics*, vol. 14, no. 1, pp. 1-10, 2023. [88] N. Nishizawa, B. Al-Qadiri, and T. Kuchimaru, "Circular polarization DOCP values for cancer identification," *Journal of Biophotonics*, vol. 14, no. 1, pp. 1-10, 2023. [89] N. Nishizawa, B. Al-Qadiri, and T. Kuchimaru, "Circular polarization DOCP values for cancer identification," *Journal of Biophotonics*, vol. 14, no. 1, pp. 1-10, 2023. [90] N. Nishizawa, B. Al-Qadiri, and T. Kuchimaru, "Circular polarization DOCP values for cancer identification," *Journal of Biophotonics*, vol. 14, no. 1, pp. 1-10, 2023. [91] N. Nishizawa, B. Al-Qadiri, and T. Kuchimaru, "Circular polarization DOCP values for cancer identification," *Journal of Biophotonics*, vol. 14, no. 1, pp. 1-10, 2023. [92] N. Nishizawa, B. Al-Qadiri, and T. Kuchimaru, "Circular polarization DOCP values for cancer identification," *Journal of Biophotonics*, vol. 14, no. 1, pp. 1-10, 2023. [93] N. Nishizawa, B. Al-Qadiri, and T. Kuchimaru, "Circular polarization DOCP values for cancer identification," *Journal of Biophotonics*, vol. 14, no. 1, pp. 1-10, 2023. [94] N. Nishizawa, B. Al-Qadiri, and T. Kuchimaru, "Circular polarization DOCP values for cancer identification," *Journal of Biophotonics*, vol. 14, no. 1, pp. 1-10, 2023. [95] N. Nishizawa, B. Al-Qadiri, and T. Kuchimaru, "Circular polarization DOCP values for cancer identification," *Journal of Biophotonics*, vol. 14, no. 1, pp. 1-10, 2023. [96] N. Nishizawa, B. Al-Qadiri, and T. Kuchimaru, "Circular polarization DOCP values for cancer identification," *Journal of Biophotonics*, vol. 14, no. 1, pp. 1-10, 2023. [97] N. Nishizawa, B. Al-Qadiri, and T. Kuchimaru, "Circular polarization DOCP values for cancer identification," *Journal of Biophotonics*, vol. 14, no. 1, pp. 1-10, 2023. [98] N. Nishizawa, B. Al-Qadiri, and T. Kuchimaru, "Circular polarization DOCP values for cancer identification," *Journal of Biophotonics*, vol. 14, no. 1, pp. 1-10, 2023. [99] N. Nishizawa, B. Al-Qadiri, and T. Kuchimaru, "Circular polarization DOCP values for cancer identification," *Journal of Biophotonics*, vol. 14, no. 1, pp. 1-10, 2023. [100] N. Nishizawa, B. Al-Qadiri, and T. Kuchimaru, "Circular polarization DOCP values for cancer identification," *Journal of Biophotonics*, vol. 14, no. 1, pp. 1-10, 2023. [101] N. Nishizawa, B. Al-Qadiri, and T. Kuchimaru, "Circular polarization DOCP values for cancer identification," *Journal of Biophotonics*, vol. 14, no. 1, pp. 1-10, 2023. [102] N. Nishizawa, B. Al-Qadiri, and T. Kuchimaru, "Circular polarization DOCP values for cancer identification," *Journal of Biophotonics*, vol. 14, no. 1, pp. 1-10, 2023. [103] N. Nishizawa, B. Al-Qadiri, and T. Kuchimaru, "Circular polarization DOCP values for cancer identification," *Journal of Biophotonics*, vol. 14, no. 1, pp. 1-10, 2023. [104] N. Nishizawa, B. Al-Qadiri, and T. Kuchimaru, "Circular polarization DOCP values for cancer identification," *Journal of Biophotonics*, vol. 14, no. 1, pp. 1-10, 2023. [105] N. Nishizawa, B. Al-Qadiri, and T. Kuchimaru, "Circular polarization DOCP values for cancer identification," *Journal of Biophotonics*, vol. 14, no. 1, pp. 1-10, 2023. [106] N. Nishizawa, B. Al-Qadiri, and T. Kuchimaru, "Circular polarization DOCP values for cancer identification," *Journal of Biophotonics*, vol. 14, no. 1, pp. 1-10, 2023. [107] N. Nishizawa, B. Al-Qadiri, and T. Kuchimaru, "Circular polarization DOCP values for cancer identification," *Journal of Biophotonics*, vol. 14, no. 1, pp. 1-10, 2023. [108] N. Nishizawa, B. Al-Qadiri, and T. Kuchimaru, "Circular polarization DOCP values for cancer identification," *Journal of Biophotonics*, vol. 14, no. 1, pp. 1-10, 2023. [109] N. Nishizawa, B. Al-Qadiri, and T. Kuchimaru, "Circular polarization DOCP values for cancer identification," *Journal of Biophotonics*, vol. 14, no. 1, pp. 1-10, 2023. [110] N. Nishizawa, B. Al-Qadiri, and T. Kuchimaru, "Circular polarization DOCP values for cancer identification," *Journal of Biophotonics*, vol. 14, no. 1, pp. 1-10, 2023. [111] N. Nishizawa, B. Al-Qadiri, and T. Kuchimaru, "Circular polarization DOCP values for cancer identification," *Journal of Biophotonics*, vol. 14, no. 1, pp. 1-10, 2023. [112] N. Nishizawa, B. Al-Qadiri, and T. Kuchimaru, "Circular polarization DOCP values for cancer identification," *Journal of Biophotonics*, vol. 14, no. 1, pp. 1-10, 2023. [113] N. Nishizawa, B. Al-Qadiri, and T. Kuchimaru, "Circular polarization DOCP values for cancer identification," *Journal of Biophotonics*, vol. 14, no. 1, pp. 1-10, 2023. [114] N. Nishizawa, B. Al-Qadiri, and T. Kuchimaru, "Circular polarization DOCP values for cancer identification," *Journal of Biophotonics*, vol. 14, no. 1, pp. 1-10, 2023. [115] N. Nishizawa, B. Al-Qadiri, and T. Kuchimaru, "Circular polarization DOCP values for cancer identification," *Journal of Biophotonics*, vol. 14, no. 1, pp. 1-10, 2023. [116] N. Nishizawa, B. Al-Qadiri, and T. Kuchimaru, "Circular polarization DOCP values for cancer identification," *Journal of Biophotonics*, vol. 14, no. 1, pp. 1-10, 2023. [117] N. Nishizawa, B. Al-Qadiri, and T. Kuchimaru, "Circular polarization DOCP values for cancer identification," *Journal of Biophotonics*, vol. 14, no. 1, pp. 1-10, 2023. [118] N. Nishizawa, B. Al-Qadiri, and T. Kuchimaru, "Circular polarization DOCP values for cancer identification," *Journal of Biophotonics*, vol. 14, no. 1, pp. 1-10, 2023. [119] N. Nishizawa, B. Al-Qadiri, and T. Kuchimaru, "Circular polarization DOCP values for cancer identification," *Journal of Biophotonics*, vol. 14, no. 1, pp. 1-10, 2023. [120] N. Nishizawa, B. Al-Qadiri, and T. Kuchimaru, "Circular polarization DOCP values for cancer identification," *Journal of Biophotonics*, vol. 14, no. 1, pp. 1-10, 2023. [121] N. Nishizawa, B. Al-Qadiri, and T. Kuchimaru, "Circular polarization DOCP values for cancer identification," *Journal of Biophotonics*, vol. 14, no. 1, pp. 1-10, 2023. [122] N. Nishizawa, B. Al-Qadiri, and T. Kuchimaru, "Circular polarization DOCP values for cancer identification," *Journal of Biophotonics*, vol. 14, no. 1, pp. 1-10, 2023. [123] N. Nishizawa, B. Al-Qadiri, and T. Kuchimaru, "Circular polarization DOCP values for cancer identification," *Journal of Biophotonics*, vol. 14, no. 1, pp. 1-10, 2023. [124] N. Nishizawa, B. Al-Qadiri, and T. Kuchimaru, "Circular polarization DOCP values for cancer identification," *Journal of Biophotonics*, vol. 14, no. 1, pp. 1-10, 2023. [125] N. Nishizawa, B. Al-Qadiri, and T. Kuchimaru, "Circular polarization DOCP values for cancer identification," *Journal of Biophotonics*, vol. 14, no. 1, pp. 1-10, 2023. [126] N. Nishizawa, B. Al-Qadiri, and T. Kuchimaru, "Circular polarization DOCP values for cancer identification," *Journal of Biophotonics*, vol. 14, no. 1, pp. 1-10, 2023. [127] N. Nishizawa, B. Al-Qadiri, and T. Kuchimaru, "Circular polarization DOCP values for cancer identification," *Journal of Biophotonics*, vol. 14, no. 1, pp. 1-10, 2023. [128] N. Nishizawa, B. Al-Qadiri, and T. Kuchimaru, "Circular polarization DOCP values for cancer identification," *Journal of Biophotonics*, vol. 14, no. 1, pp. 1-10, 2023. [129] N. Nishizawa, B. Al-Qadiri, and T. Kuchimaru, "Circular polarization DOCP values for cancer identification," *Journal of Biophotonics*, vol. 14, no. 1, pp. 1-10, 2023. [130] N. Nishizawa, B. Al-Qadiri, and T. Kuchimaru, "Circular polarization DOCP values for cancer identification," *Journal of Biophotonics*, vol. 14

「一回目で感じた疑問」 やよく分からなかった 点を一日調べてみ から2回目を読む

Angular optimization for cancer identification with
Nozomi Nishizawa, Basam Al-Qadiri, Takahiro Kuchimaru
Point-to-point
Circular polarization
Multiple scattering
Optical biopsy
Tissue sample

Keywords: circular polarization, multiple scattering, optical biopsy, tissue sample

1 | INTRODUCTION

The multiple scattering phenomenon of polarized light provides valuable information regarding scattering in a turbid material, based on the polarization state as well as the remanent intensity of the scattered light. When polarized light beams impinge on a biological tissue, they penetrate and propagate into the tissue and are scattered multiple times by cell nuclei, which are the main

scattering in biological tissues. Eventually, they are absorbed and/or discharged outside the tissue. Depolarization of the resultant scattered light mainly depends on the size and axial ratio of scatterers, that is, cell nuclei, as well as the frequency of scattering events associated with the density and distribution of cell nuclei.

Rickett et al [1] reported that the polarization state of light is scattered differently from suspended biological scatterers as well as cell nuclei, which are the main

scattering in biological tissues. Eventually, they are absorbed and/or discharged outside the tissue. Depolarization of the resultant scattered light mainly depends on the size and axial ratio of scatterers, that is, cell nuclei, as well as the frequency of scattering events associated with the density and distribution of cell nuclei.

Rickett et al [1] reported that the polarization state of light is scattered differently from suspended biological scatterers as well as cell nuclei, which are the main

scattering in biological tissues. Eventually, they are absorbed and/or discharged outside the tissue. Depolarization of the resultant scattered light mainly depends on the size and axial ratio of scatterers, that is, cell nuclei, as well as the frequency of scattering events associated with the density and distribution of cell nuclei.

Rickett et al [1] reported that the polarization state of light is scattered differently from suspended biological scatterers as well as cell nuclei, which are the main

scattering in biological tissues. Eventually, they are absorbed and/or discharged outside the tissue. Depolarization of the resultant scattered light mainly depends on the size and axial ratio of scatterers, that is, cell nuclei, as well as the frequency of scattering events associated with the density and distribution of cell nuclei.

Rickett et al [1] reported that the polarization state of light is scattered differently from suspended biological scatterers as well as cell nuclei, which are the main

scattering in biological tissues. Eventually, they are absorbed and/or discharged outside the tissue. Depolarization of the resultant scattered light mainly depends on the size and axial ratio of scatterers, that is, cell nuclei, as well as the frequency of scattering events associated with the density and distribution of cell nuclei.

Rickett et al [1] reported that the polarization state of light is scattered differently from suspended biological scatterers as well as cell nuclei, which are the main

scattering in biological tissues. Eventually, they are absorbed and/or discharged outside the tissue. Depolarization of the resultant scattered light mainly depends on the size and axial ratio of scatterers, that is, cell nuclei, as well as the frequency of scattering events associated with the density and distribution of cell nuclei.

Rickett et al [1] reported that the polarization state of light is scattered differently from suspended biological scatterers as well as cell nuclei, which are the main

scattering in biological tissues. Eventually, they are absorbed and/or discharged outside the tissue. Depolarization of the resultant scattered light mainly depends on the size and axial ratio of scatterers, that is, cell nuclei, as well as the frequency of scattering events associated with the density and distribution of cell nuclei.

Rickett et al [1] reported that the polarization state of light is scattered differently from suspended biological scatterers as well as cell nuclei, which are the main

scattering in biological tissues. Eventually, they are absorbed and/or discharged outside the tissue. Depolarization of the resultant scattered light mainly depends on the size and axial ratio of scatterers, that is, cell nuclei, as well as the frequency of scattering events associated with the density and distribution of cell nuclei.

Rickett et al [1] reported that the polarization state of light is scattered differently from suspended biological scatterers as well as cell nuclei, which are the main

scattering in biological tissues. Eventually, they are absorbed and/or discharged outside the tissue. Depolarization of the resultant scattered light mainly depends on the size and axial ratio of scatterers, that is, cell nuclei, as well as the frequency of scattering events associated with the density and distribution of cell nuclei.

Rickett et al [1] reported that the polarization state of light is scattered differently from suspended biological scatterers as well as cell nuclei, which are the main

scattering in biological tissues. Eventually, they are absorbed and/or discharged outside the tissue. Depolarization of the resultant scattered light mainly depends on the size and axial ratio of scatterers, that is, cell nuclei, as well as the frequency of scattering events associated with the density and distribution of cell nuclei.

Rickett et al [1] reported that the polarization state of light is scattered differently from suspended biological scatterers as well as cell nuclei, which are the main

scattering in biological tissues. Eventually, they are absorbed and/or discharged outside the tissue. Depolarization of the resultant scattered light mainly depends on the size and axial ratio of scatterers, that is, cell nuclei, as well as the frequency of scattering events associated with the density and distribution of cell nuclei.

Rickett et al [1] reported that the polarization state of light is scattered differently from suspended biological scatterers as well as cell nuclei, which are the main

scattering in biological tissues. Eventually, they are absorbed and/or discharged outside the tissue. Depolarization of the resultant scattered light mainly depends on the size and axial ratio of scatterers, that is, cell nuclei, as well as the frequency of scattering events associated with the density and distribution of cell nuclei.

Rickett et al [1] reported that the polarization state of light is scattered differently from suspended biological scatterers as well as cell nuclei, which are the main

scattering in biological tissues. Eventually, they are absorbed and/or discharged outside the tissue. Depolarization of the resultant scattered light mainly depends on the size and axial ratio of scatterers, that is, cell nuclei, as well as the frequency of scattering events associated with the density and distribution of cell nuclei.

Rickett et al [1] reported that the polarization state of light is scattered differently from suspended biological scatterers as well as cell nuclei, which are the main

biological tissue. They suggested that this technique is useful for distinguishing closely related structural biological systems and for identifying subsequent time-dependent structural changes. Most of the earlier studies that were conducted to observe biological structures with the polarization state of the back-scattered light have been performed using the linear polarized (LP) light [2–8]. In the Mie scattering regime [9], the size of a scatterer (cell nucleus) is larger than the wavelength of incident light, and the degree of polarization for LP light is significantly large such that the scattered light results in complete depolarization by a small number of scattering events [10, 11]. Therefore, these studies using LP light have successfully provided scientific significance specifically for surface observation [12–14].

In contrast, the circular polarization of light has more persistence against multiple scattering in the Mie regime. The depolarization process is caused by two randomized processes: rotation of the polarization plane and interference with the backscattered light. When the size of a scatterer is almost equivalent or smaller than the wavelength of incident light (Rayleigh regime), LP light is randomized mostly by the former process, whereas circularly polarized (CP) light is classified dominantly by the latter process. The strength of the resultant depolarization was almost equivalent. In the Mie regime, in which forward scattering is dominant [9], complete depolarization of CP light requires more scattering events compared with those of LP light owing to the reduction in the backward scattering [10, 11]. Therefore, scattering of CP light can provide more specific information about not only the contoured surface but also the interior of tissues, which suggests the possibility of identifying cancerous tissues in vivo.

Magnaki et al [15] pioneered the application of CP light for cancer detection by experimentally measuring the scattering properties of tissues on the Polaroid scope. Kumen et al [16] reported that the polarization of light scattered from a tissue of human lung shows different polarization states for healthy and tumor tissues as vivo using incident CP light ($\lambda = 633 \text{ nm}$). They concluded that the difference in polarization is caused by the enlargement of the nucleus size due to cancerization. Furthermore, they suggested that this technique would generate noninvasive diagnostic technology for early disease detection. Triggered by these reports, the tissue polarization technique has been widely applied to develop an optical diagnostic tool that can provide supplementary information for pathologists [17–24]. Recently, the polarimetry technique has been applied and demonstrated for grading colon cancer [21] and Alzheimer's disease [25].

We have studied spin-polarizing light-emitting diodes (spin-LEDs) that can emit fully CP light directly from the side facet and can detect CP light without applying an external magnetic field or a large electrical field [26–30]. If spin-LED devices are integrated at the top of a biopsy probe apparatus such as an endoscope, the polarimetry technique suggested by Magnaki et al can be developed from ex vivo observation to in vivo observation, which can enable observation in real time while avoiding the risk of administering a fluorescent agent. However, to develop this technique for practical use, more intensive and detailed investigations are required from both theoretical and experimental approaches.

Previously, we theoretically investigated the scattering process of CP light against cell nuclei in pseudo tissue using Monte Carlo (MC) simulations based on the Mie scattering mechanism [31]. MC simulations were performed for cancerous and healthy pseudo tissues in aqueous medium containing dispersed particles with the typical size of cell nuclei in healthy and cancerous cells, that is, 6 and 11 μm , respectively. Accordingly, a distinct difference in the resultant polarization values between healthy and cancerous tissues can be obtained over a wide range of detection angles, which suggests that this technique can characterize the size of cell nuclei in biological tissues. The difference is estimated to be approximately 0.2 in the degree of circular polarization (DOCP) values.

In this study, we experimentally demonstrated the identification of cancer in blood vessel-like tissue with the scattering of CP light. We measured the DOCP values of scattered light in various optical arrangements with incident and detection angles. Line-scanning experiments were performed to demonstrate clear discrimination of the cancerous and healthy parts, which was partially published in ref. [32]. In addition, we assessed the in-phase dispersion of the detected values according to optical angular configurations.

2 | EXPERIMENTAL

Figure 1A shows the experimental setup used to measure the DOCP values in this study. The incident and detection angles θ_i and θ_d are defined as angles made by the lines connecting from a measurement point on the sample to the light source and the detector with a perpendicular line at the measurement point, respectively. The unpolarized laser beam (633 nm) is emitted from a fiber-optic probe (Sanctus Laser Technology Co., Ltd., China) with a wavelength of 914 nm and a power of 100 mW was converted to the right-handed CP light with 633 nm through an ND filter, a linear polarizer and a quarter-wave ($\lambda/4$) plate Subsequently, the CP light is incident on the specimen (with $F = 25 \text{ mm}$) at a measurement point with an incident angle θ_i . The DOCP value of the incident CP light was

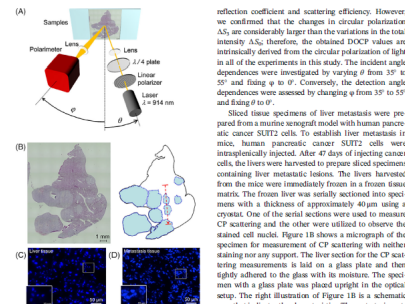


FIGURE 1 A. Schematic illustration of experimental setup for measuring the degree of circular polarization (DOCP) value in the study. B. DOCP micrograph of specimen and right) corresponding schematics map. The light-blue areas delineated by the red dot-line represent the metastatic parts on the live dot-line representing the metastatic parts. The red dot-line areas show the healthy parts. The scattered light measurements were performed, which is shown normal and metastatic parts. Fluorescence micrographs of C: healthy liver cell and D: cancerous liver cell. The scattered light measurements are shown in Figure 1C, D, respectively. The liver sections were fixed with 4% paraformaldehyde for 10 minutes. The metastatic parts were stained with hematoxylin and eosin (H&E) stain. The fixed sections were stained with 10 μm Hoechst 33254 for 5 minutes. The stained sections were sealed with cover slips and fluorescently observed with an inverted fluorescence microscope (Olympus, Keyence) Fluorescence images and DOCP micrographs were obtained from the same area of the CMOS camera. The cell nuclei in the healthy part are comparatively small and dispersed, and the average diameter of the cell nuclei is approximately 6.4 μm . In the metastatic part, relatively large and aggregated cell nuclei are observed, which indicate that the DOCP values are scattered differently from the healthy parts due to cancerization. The average diameter of the cell nuclei is approximately 11 μm .

~ 10 . The scattered light from the sample at an angle of $\theta_d = 5.7^\circ$ is collected by a lens (radius of $R = 20 \text{ mm}$, and light detected by a photomultiplier tube under fast exposure time of the CMOS camera. The cell nuclei in the healthy part are comparatively small and dispersed, and the average diameter of the cell nuclei is approximately 6.4 μm . In the metastatic part, relatively large and aggregated cell nuclei are observed, which indicate that the DOCP values are scattered differently from the healthy parts due to cancerization. The average diameter of the cell nuclei is approximately 11 μm .

MC simulations for the pseudo-biological tissue with a thickness of 40 μm show that the sampling volume is

approximately 1 mm \times 1 mm \times 40 μm , independent of the angular configurations. The sampling depth at $(\theta_i = 6^\circ, \theta_d = 1^\circ, 30^\circ)$ is estimated to be 1.65 mm from the MC calculations for the tissue with infinite thickness [31]. Therefore, a significant portion of incident light is transmitted through the back of the sample or reflected at the interface between the specimen and the glass plate. The remaining portion of light and reflected light at the back undergo multiple scattering events in the entire sample with a thickness of 40 μm and then arrive at the detector. This sampling volume includes approximately 750 nuclei on average.

3 | RESULTS AND DISCUSSION

Figure 2A,B shows the dependence of the DOCP value of scattered light on the incident angle θ_i and detection angle θ_d , respectively. The blue and red dots and lines represent the DOCP values measured at the point in the reflection (ray) support.

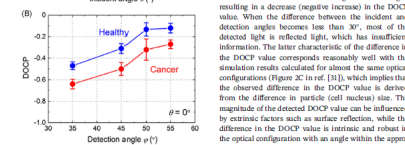


FIGURE 2 Degree of circular polarization (DOCP) values as a function of A: incident angle θ_i with $\theta_d = 0^\circ$ and B: detection angle θ_d with $\theta_i = 0^\circ$, respectively

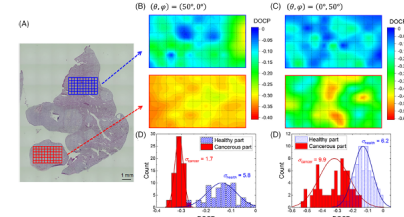


FIGURE 4 Results of the scanning measurements. A: The measured areas of healthy and cancerous parts, delineated by blue and red squares, respectively, on the micrograph of specimen. B,C: The color-coded spatial distributions of the measured degree of circular polarization (DOCP) values for upper pseudo healthy and lower pseudo cancerous parts with $\theta_i = 0^\circ$ and $\theta_d = 0^\circ$ ($0^\circ, 5^\circ, 10^\circ$), respectively. D,E: Histograms of the DOCP values shown in B, and C, respectively, together with the overlaid distribution curves and the standard deviation values.

optical configurations with oblique incidence and vertical detection have less spatial resolution. From the results of line-scanning experiments, the in-plane results are roughly estimated to be 0.4 and 0.3 mm for the configurations with the oblique and perpendicular incidence, respectively.

To evaluate the distributions of the DOCP values, scanning measurements were performed in an area that appeared different shown on the micrograph of the specimen in Figure 4A. The color-coded spatial distributions of the measured DOCP values on the area of $(\theta_i = 0^\circ, \theta_d = 0^\circ)$ are shown in Figure 4B, respectively. The upper pseudo shows the data in the healthy tissues, while the lower pseudo shows the data in the cancerous tissues. The different color histograms of the DOCP values corresponding to the data shown in Figure 4B,C, respectively. At $(\theta_i = 0^\circ, \theta_d = 0^\circ)$, the dispersion of the DOCP values in the cancerous part is characterized with a peak of ~ 0.4137 and a standard deviation of $\sigma = 0.58$, whereas the DOCP values in the cancerous part are averaged at ~ 0.31 with a standard deviation of $\sigma = 0.49$ (Figure 4B,D). The almost independent dispersion provide

4 | CONCLUSION

We experimentally investigated the applicability of scattered CP light for cancer identification in optical

configurations with various angular relations between the direction of incidence and detection. An incident angle larger than the Brewster angle for the surface of biological tissue causes a decrease in polarization of the scattered light. In addition, the DOCP values depend on the angles of incidence and detection increases surface reflection with less information. At the configurations with angles within the appropriate range, that is, $\theta_i \leq 5^\circ$ and $(\theta_i - \theta_d) \leq 30^\circ$, the significance differences between the DOCP values obtained from the cancerous and healthy parts are observed to be approximately 0.2, which is sufficient to identify the cancer-affected area. Based on the good agreement with our previous calculation in [31], here, we concluded that the difference in the DOCP values results from the different sizes of cell nuclei rather than the different refractive indices, which suggests that this technique could be applied to the identification of not only cancerous but also other diseases characterized by the enlargement of cell nuclei, for example, alcoholic hepatitis and cirrhosis of the liver. In addition to the cell nuclei, the combination of cellular walls and other constituents also contributes to polarization scattering. These components, which are strongly associated with the anisotropic cellular shape and structures, can greatly contribute to polarization scattering in the tissue, asymmetric complex tissue, and a tissue in which isotropic mutation is observed. The samples used in this study consist of normal, isotropic cell nuclei in both cancerous and healthy tissues, in which the contributions of these isotropic parameters are inconspicuous. Further research is required to investigate these differences. In the line-scanning experiments, the obtained results are sensitive to the detection angle, which depends on the state of tissue, whether healthy or cancerous. The optical configuration with a large detection angle provides larger differences in the DOCP values, which indicate higher accuracy in identifying cancerous parts. However, the large detection angle is not always available due to the scattering losses of light and the detection angle reduces the spatial resolution and enhances the positional fluctuation. Conversely, the arrangements with perpendicular incidence and light detection provide higher accuracy due to a narrow sampling volume but slightly less accuracy due to fewer scattering events. These arrangements should be selected according to the objectives, such as organ, apparatus and environment. Moreover, an analysis of the difference in the DOCP values obtained on the same configuration with angles within the appropriate range, which makes it permissible to include the DOCP values in the multiple-parameter-based diagnosis system. This indicates that this technique is useful even in environments where it is difficult to fix the spatial arrangement between the light source and the target, such as in vivo observation with an endoscope.

AUTHOR BIOGRAPHIES

Point-to-point
Circular polarization
Multiple scattering
Optical biopsy
Tissue sample

Keywords: circular polarization, multiple scattering, optical biopsy, tissue sample

Keywords: circular polarization, multiple scattering, optical biopsy, tissue sample

Keywords: circular polarization, multiple scattering, optical biopsy, tissue sample

Keywords: circular polarization, multiple scattering, optical biopsy, tissue sample

Keywords: circular polarization, multiple scattering, optical biopsy, tissue sample

Keywords: circular polarization, multiple scattering, optical biopsy, tissue sample

Keywords: circular polarization, multiple scattering, optical biopsy, tissue sample

Keywords: circular polarization, multiple scattering, optical biopsy, tissue sample

3 | RESULTS AND DISCUSSION

Figure 2A,B shows the dependence of the DOCP value of scattered light on the incident angle θ_i and detection angle θ_d , respectively. The blue and red dots and lines represent the DOCP values measured at the point in the reflection (ray) support.

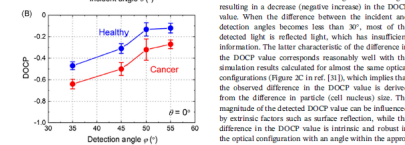


FIGURE 2 Degree of circular polarization (DOCP) values as a function of A: incident angle θ_i with $\theta_d = 0^\circ$ and B: detection angle θ_d with $\theta_i = 0^\circ$, respectively

configurations with various angular relations between the direction of incidence and detection. An incident angle larger than the Brewster angle for the surface of biological tissue causes a decrease in polarization of the scattered light. In addition, the DOCP values depend on the angles of incidence and detection increases surface reflection with less information. At the configurations with angles within the appropriate range, that is, $\theta_i \leq 5^\circ$ and $(\theta_i - \theta_d) \leq 30^\circ$, the significance differences between the DOCP values obtained from the cancerous and healthy parts are observed to be approximately 0.2, which is sufficient to identify the cancer-affected area. Based on the good agreement with our previous calculation in [31], here, we concluded that the difference in the DOCP values results from the different sizes of cell nuclei rather than the different refractive indices, which suggests that this technique could be applied to the identification of not only cancerous but also other diseases characterized by the enlargement of cell nuclei, for example, alcoholic hepatitis and cirrhosis of the liver. In addition to the cell nuclei, the combination of cellular walls and other constituents also contributes to polarization scattering. These components, which are strongly associated with the anisotropic cellular shape and structures, can greatly contribute to polarization scattering in the tissue, asymmetric complex tissue, and a tissue in which isotropic mutation is observed. The samples used in this study consist of normal, isotropic cell nuclei in both cancerous and healthy tissues, in which the contributions of these isotropic parameters are inconspicuous. Further research is required to investigate these differences. In the line-scanning experiments, the obtained results are sensitive to the detection angle, which depends on the state of tissue, whether healthy or cancerous. The optical configuration with a large detection angle provides larger differences in the DOCP values, which indicate higher accuracy in identifying cancerous parts. However, the large detection angle is not always available due to the scattering losses of light and the detection angle reduces the spatial resolution and enhances the positional fluctuation. Conversely, the arrangements with perpendicular incidence and light detection provide higher accuracy due to a narrow sampling volume but slightly less accuracy due to fewer scattering events. These arrangements should be selected according to the objectives, such as organ, apparatus and environment. Moreover, an analysis of the difference in the DOCP values obtained on the same configuration with angles within the appropriate range, which makes it permissible to include the DOCP values in the multiple-parameter-based diagnosis system. This indicates that this technique is useful even in environments where it is difficult to fix the spatial arrangement between the light source and the target, such as in vivo observation with an endoscope.

AUTHOR BIOGRAPHIES

Point-to-point
Circular polarization
Multiple scattering
Optical biopsy
Tissue sample

Keywords: circular polarization, multiple scattering, optical biopsy, tissue sample

Keywords: circular polarization, multiple scattering, optical biopsy, tissue sample

Keywords: circular polarization, multiple scattering, optical biopsy, tissue sample

Keywords: circular polarization, multiple scattering, optical biopsy, tissue sample

Keywords: circular polarization, multiple scattering, optical biopsy, tissue sample

Keywords: circular polarization, multiple scattering, optical biopsy, tissue sample

Keywords: circular polarization, multiple scattering, optical biopsy, tissue sample

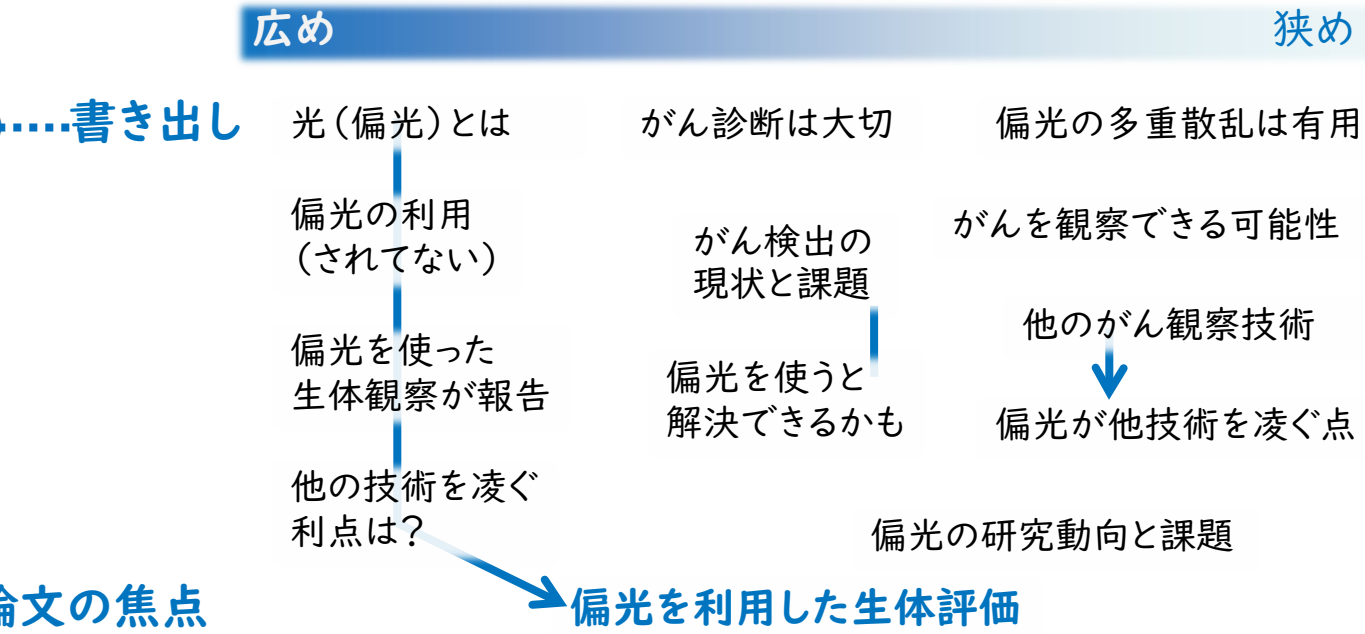
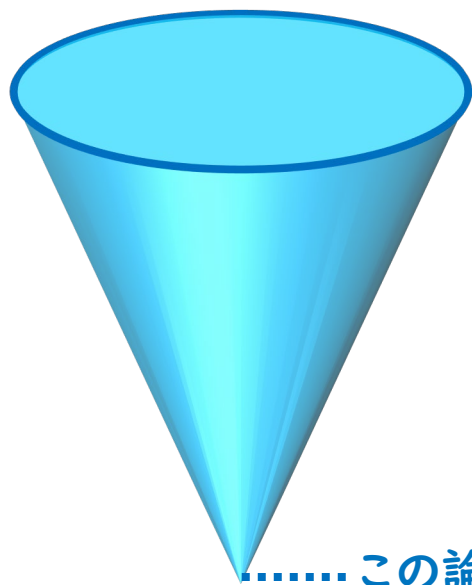
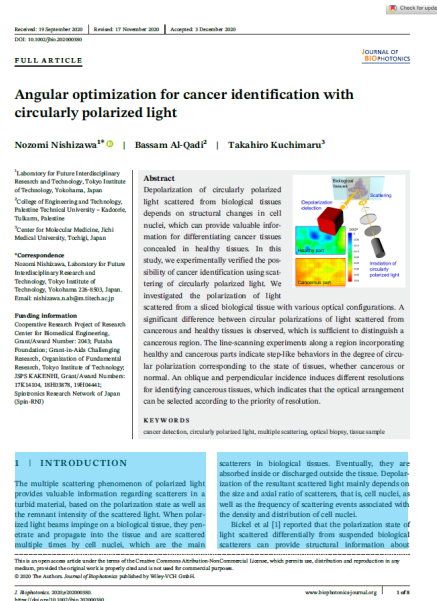
Keywords: circular polarization, multiple scattering, optical biopsy, tissue sample

How to cite this article: Nishizawa N, Al-Qadiri B, Kuchimaru T. Angular optimization for cancer identification with circularly polarized light. *J Biophotonics*. 2020;13(10):20200008. <https://doi.org/10.1002/jbip.20200008>

各部の読み方 Introduction

Introductionは一般に広いところから狭いところへ、そしてこの論文の焦点のところまで話の焦点を絞っていくように書かれている

研究の歴史や既存技術や対抗技術・手法・材料の研究動向や利点・問題点などを整理してくれている場合もあるので研究全体の流れを捉えるのに便利。この部分の参考文献は把握しておくべき



各部の読み方 Conclusion

Conclusion部は SummaryとConclusion(Message)からなる

Summaryはこれまでの内容のまとめ (この部分に初見の内容は書かれない)

- 研究目的
- 研究手法と内容、結果
- それぞれの結果に対する考察

discussionでは複雑・難解だが、ここでは簡素に書かれるので読みやすくなっている

Conclusionは著者が読者に向けたMessageに相当する

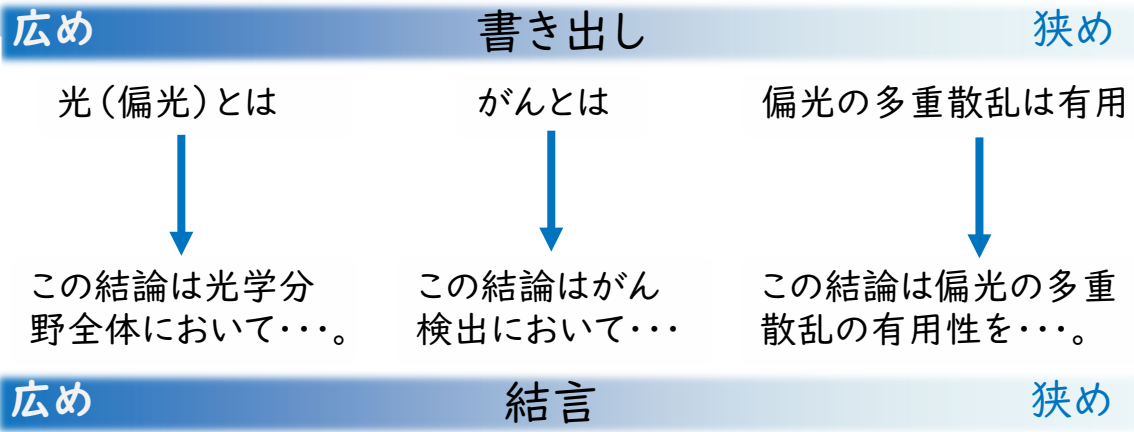
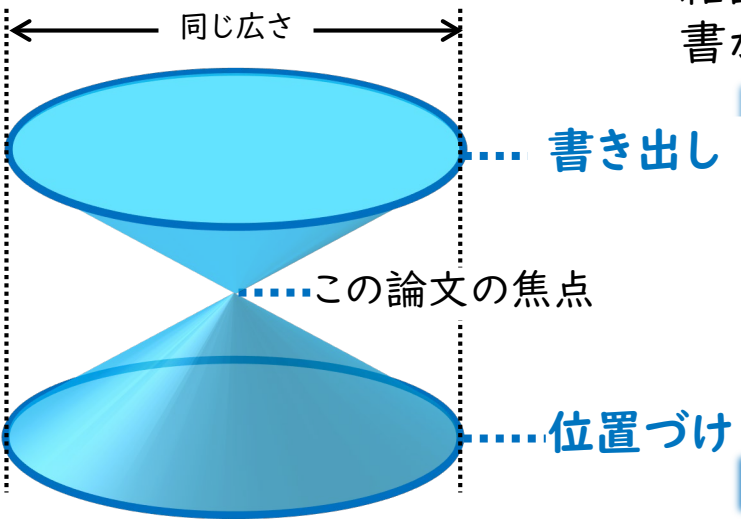
- 考察を集約して導き出された結論
- この結論の研究全体における位置づけ(結言)

configurations with various angular relations between the direction of incidence and detection. An incident angle larger than the Brewster's angle for the surface of biological tissues causes a decreased penetration of polarized light into the tissue, and the small difference between the angles of incidence and detection increases surface reflection with less information. At the configuration with angles within the appropriate range, that is, $\theta \leq 53^\circ$ and $(\theta - \varphi) \geq 30^\circ$, the significant differences between the DOCP values obtained from the cancerous and healthy parts are observed to be approximately 0.26, which is sufficient to identify the cancer-affected area. Based on the good agreement with our previous calculation [11], here, we concluded that the difference in the DOCP values results from the different sizes of cell nuclei rather than the different reflectance values, which suggests that this technique could be applied to the identification of not only carcinoma but also other diseases accompanied by the enlargement of cell nuclei, for example, alcoholic hepatitis and ulcerous colitis. In addition to the cell nuclei, the contribution of cellular walls and other constituents also contributes to polarization scattering. These components, which are strongly associated with the anisotropic cellular shape and birefringence, can greatly contribute to polarization scattering in fibrous tissue, asymmetric complex tissue, and a tissue in which anisotropic mutation is observed. The samples used in this study consist of uniform, isotropic cell nuclei in both cancerous and healthy parts, in which the contributions of these anisotropic parameters are inconspicuous. Further research is required to investigate these contributions. In the live-scanning measurements, the obtained DOCP values change as an almost primary manner depending on the target tissue, whether healthy or cancerous. This indicates that the DOCP values are a good indicator of higher accuracy in identifying cancerous parts. However, the elongated elliptic spot due to oblique incidence reduces the spatial resolution and enhances the positional fluctuation. Conversely, the arrangements with perpendicular incident light have higher spatial resolution due to a narrow sampling volume but slightly less accuracy due to fewer scattering events. These arrangements should be selected according to the objective disease, organ, apparatus and environment. Moreover, an almost constant difference in the DOCP values can be obtained at the configuration with angles within the appropriate range, which makes it permissible to incline the surface of measuring tissue against the fixed optical system. This indicates that this technique is useful even in environments where it is difficult to fix the spatial arrangement between the optical and the target, such as in vivo observations with an endoscope.

Conclusion

4 | CONCLUSION
We experimentally investigated the applicability of scattered CP light for cancer identification in optical

結論の位置づけは、Introductionの書き出しに対応する形で書かれるときれいにまとまった良い論文と言える



Materials and methods部は実際に行った実験や解析の手法が書かれている。

Materials部は

- 対象となる材料、検体、素子の特性
- 準備方法
- 加工方法等

Methods部は

[実験]

- 実験手法や条件、
 - 使用した装置(市販品か自作か)
 - 振ったパラメーターとその根拠
 - データ解析の手法
- [Simulationや計算]
- 計算手法、条件
 - 振ったパラメーターとその根拠
 - 得られたデータの正当性(予め示せる場合のみ)

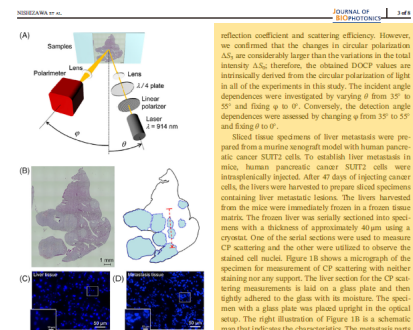


FIGURE 1 A, Schematic illustration of experimental setup for measuring the degree of circular polarization (DOCP) value in the study. B, (left) Micrograph of specimen and (right) a corresponding schematic map. The light blue area delineated by the blue dotted line represent the metastatic parts. The red dotted arrow shows the area where live-scanning experiments were performed, which is across normal and metastatic parts. Fluorescence micrographs of C, healthy liver and, D, metastatic tissue with stained cell nuclei in the specimen. The tissue show the magnified images of the region in white boxes. *1.0. The light scattered from the sample at an angle of $\theta = 5.7^\circ$ is collected by a fiber optic lens ($f = 30 \text{ mm}$) and detected by a photomultiplier tube (PMT) in the PAX1000 Thorlabs) equipped with a 10 nm bandpass filter and a laser aperture ($\lambda = 635 \text{ nm}$, $f = 10 \text{ mm}$, $\text{NA} = 0.1$) and a photodiode. The polarization state of the scattered light is assessed by the DOCP values, which is defined by the ratio of the DOCP values over the S_0 and the Stokes parameter S_2 in the detection. The average diameter of the cell nuclei is approximately $10.8 \mu\text{m}$. *1.0. The DOCP value of the incident CP light was

reflection coefficient and scattering efficiency. However, we confirmed that the changes in circular polarization AS, are considerably larger than the variations in the total intensity S_0 . Also, therefore, the observed DOCP values are intrinsically derived from the circular polarization of light in all of the experiments in this study. The incident angle dependences were investigated by varying θ from 35° to 55° and fixing ϕ to 0° . Conversely, the detection angle dependences were assessed by changing ϕ from 30° to 55° and fixing θ to 0° .

Sliced tissue specimens of liver metastasis were prepared from a murine xenograft model with human pancreatic cancer SUT2 cells. To establish liver metastasis in mice, human pancreatic cancer SUT2 cells were intraperitoneally injected. After 47 days of injecting cancer cells, the livers were harvested to prepare sliced specimens containing liver metastatic lesions. The livers harvested from the mice were immediately frozen in a frozen tissue matrix. The frozen liver was serially sectioned into specimens with a thickness of approximately $40 \mu\text{m}$ using a cryostat. One of the serial sections were used to measure CP scattering and the other were utilized to observe the stained cell nuclei. Figure 1B shows a micrograph of the specimen for measurement of CP scattering with neither staining nor any support. The liver section for the CP scattering measurement is laid on a glass plate and then tightly adhered to the glass with its moisture. The specimen with a glass plate was placed upright in the optical setup. The right illustration of Figure 1B is a schematic map that indicates the characteristic. The metastatic parts are shown by the light blue area surrounded by a dotted line. The red dotted arrow denotes the linear area along which the live-scanning measurements were performed. The fluorescence micrographs of healthy liver and metastatic area with stained cell nuclei in the specimen are shown in Figure 1C,D, respectively. The liver sections were fixed with 4% paraformaldehyde for 10 minutes. After washing with phosphate-buffered saline, the fixed sections were stained with 10 $\mu\text{g/ml}$ Hoechst 33258 for 5 minutes. The stained sections were sealed with cover slips and fluorescently observed with an inverted fluorescence microscope (IX2000, Keyence). Fluorescence images were captured with a x40 objective lens under fixed exposure. The stained cell nuclei in the specimen were observed with a 40x objective lens. The average diameter of the stained cell nuclei is approximately $10.8 \mu\text{m}$. The DOCP values were measured by the measurement of cell nuclei in observed in metastatic parts in the specimen. The average diameter of the stained cell nuclei is approximately $10.8 \mu\text{m}$. *1.0. The DOCP value of the incident CP light was

approximately $1 \text{ mm} \times 1 \text{ mm} \times 40 \mu\text{m}$, independent of the angular configurations. The sampling depth at $(\theta, \phi) = (1^\circ, 30^\circ)$ is estimated to be 1.65 mm from the MC calculations for the tissue with infinite thickness [11]. Therefore, a significant portion of incident light is transparent through the back of the sample or reflected at the interface between the specimen and the glass plate. The remaining portion of light and reflected light at the back undergo multiple scattering events in the entire sample with a thickness of $40 \mu\text{m}$ and then arrive at the detector. This sampling volume includes approximately 750 nuclei on average.

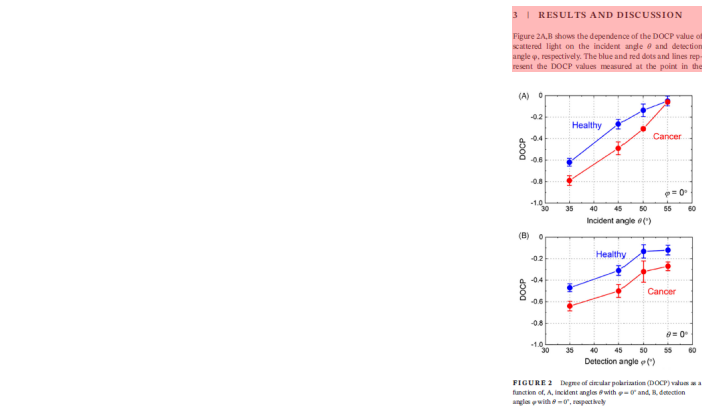
Materials and Methods

細かい記述で理解が大変ではあるが、次の結果を理解する上では重要な部分。

また、結論が正しいのかどうかを判定する、同じ(様な)実験をする等の場合には一字一句よく読み込む必要がある

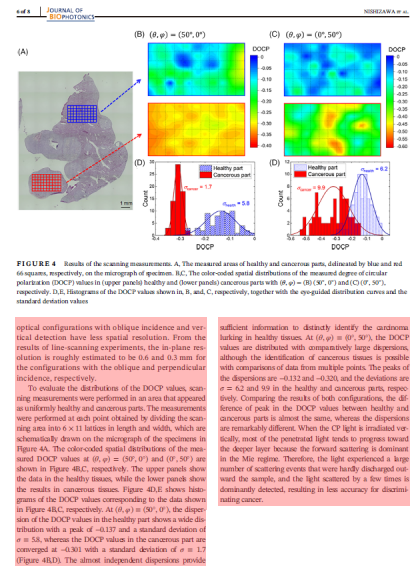
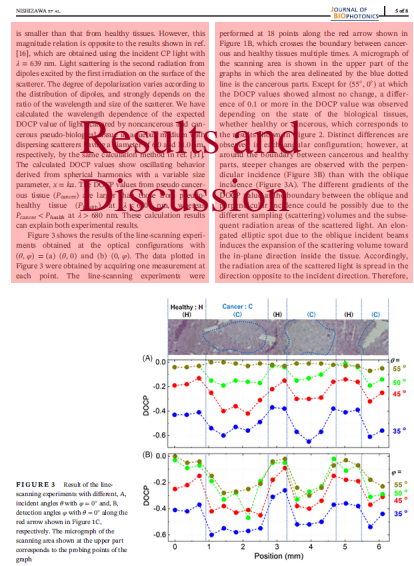
Nature系などは論文の最後の方にまとめられていたり、補足資料(Supplementary materials)に入れられている論文誌もある

Results and Discussion部は
文字通り結果と考察について
書かれている



is smaller than that from healthy tissues. However, this magnified relation is opposite to the results shown in ref. [36], which are obtained using the incident CP light with $\lambda = 639$ nm. Light scattering is the second radiation from the dipoles excited by the first irradiation on the surface of the scatterer. The degree of depolarization varies according to the distribution of dipoles, and strongly depends on the ratio of the wavelength and size of the scatterer. We have calculated the wavelength dependence of the expected DOCP value of light scattered by noncancerous and cancerous pseudo-brain tissues (Figure 2). Distinct differences are appearing scattered light between cancerous and healthy tissues (Figure 2). The calculated DOCP values show oscillating behavior derived from spherical harmonics with a variable scattering parameter, $x = ka$, where k is the wave number of the incident wave ($P_{\text{max}} = 0.6$) and a is the radius of the scatterer ($P_{\text{max}} < P_{\text{max}}$ at $\lambda > 600$ nm). These calculation results can explain both experimental results.

Figure 3 shows the results of the line-scanning experiments obtained at the optical configurations with $(\theta, \phi) = (0, 0)$ and $(0, 90)$ (see the data plotted in Figure 3) were obtained by acquiring one measurement at each point. The line-scanning experiments were



(Result → Discussion) × n

または
Results → Discussion 見出しで分けられている
という構成のどちらかが多い

Results部は
得られた結果を示した図、グラフ、画像に
対しての説明を中心にかかかれているため、
比較的理解しやすい

Discussion部は
得られた結果の解釈、著者の考察が書か
れている論文でいちばん重要な部分

結果の位置づけや解釈の他、今後の展望
や今回はできなかった部分なども書かれ
ることがあるので、読者にとっては有益な
こともある

根拠となる参考文献のうち重要と考えら
れるものをリスト化しておく

各部の読み方 References

References (引用文献)

本文中で引用、または参考にした論文のリスト(すべてを読む必要はないが重要なものは目を通す必要がある)

Introductionに紐づけされた引用文献

その研究に至った歴史の部分においてはマイルストーンとなる論文を順に挙げていることが多いので、次に読む論文を探す場合などはここまた、焦点の絞り具合によって、より広い領域の重要論文などが挙げられており、必要とする段階に応じて目を通す必要がある

Materials and Methodsに紐づけされた引用文献

同様の試料や手法を使った実験、手法そのものについての論文などもある

Results and Discussionに紐づけされた引用文献

考察の根拠などに関しての引用の場合、詳細が書かれている場合もある

Conclusionsに紐づけされた引用文献

今後の展望の部分では次の研究の指標になる論文が挙げられている場合もある

※ 本論文と著者が同じなのか違うのかによって意味合いが変わることがあるので注意

REFERENCES

- [1] W. S. Rickel, J. F. Davidson, D. R. Huffman, R. Kikhan, *Proc Natl Acad Sci U S A* **1976**, *73*, 486.
- [2] V. Beckman, R. George, K. Radhakrishnan, I. Rubin, R. J. D'Amico, L. T. Perelman, M. S. Feld, *IEEE J. Sel. Top. Quantum Electron.* **1995**, *1*, 619.
- [3] A. H. Hitchcock, J. R. Mourou, I. J. Bigaj, *Appl Optics* **1997**, *36*, 123.
- [4] F. Rhee-Choo, D. Laonte, R. Lamb, P. Schermerberger, S. Schell, *J. Opt. Soc. Am. A* **2004**, *21*, 1769.
- [5] R. S. George, V. Beckman, L. T. Perelman, I. Grigorovich, R. Radhakrishnan, I. Rubin, R. J. D'Amico, M. S. Feld, *Nat. Mat.* **2001**, *1*, 249.
- [6] V. V. Tuchin, L. V. Wang, D. A. Zilyakov, *Optical Polarization in Biomedical Applications*, Springer, New York, NY, **2006**.
- [7] S. Mariani, E. M. Sessa, S. H. Paol, A. Uppal, N. Ghosh, P. E. Gupta, *J. Biophotonics* **2006**, *1*, 151.
- [8] G. Chok, A. Villo, *J. Biomed Opt.* **2011**, *16*, 110101.
- [9] F. F. Reibel, D. R. Huffman, *Absorption and Scattering of Light by Small Particles*, Wiley, New York, NY, **1987**.
- [10] C. MacKintosh, J. X. Zhu, D. J. Rice, D. A. Waite, *Phys. Rev. B* **1998**, *60*, 0452.

REFERENCES

- [11] D. Biond, C. Bassano, A. S. Martinez, J. M. Schmitt, *Phys. Rev. E* **1994**, *49*, 1787.
- [12] G.M. Romagnolo, A. Scialò, M. Anzolini, T. Norkova, P. Valletta, B. Capot, A. D. Mariani, *Opt. Express* **2014**, *22*, 1342.
- [13] D.K. Papatoglu, S. Mariani, A. Scialò, C. Falcit, I. Toubantsev, R. M. Anzolini, T. Norkova, B. Capot, A. Mariani, P. Valletta, *J. Biomed Opt.* **2012**, *17*, 060301.
- [14] P. Papatoglu, A. Scialò, A. Scialò, P. Valletta, H. Cohen, T. Norkova, B. H. Dushkin, S. Mariani, C. Falcit, M.R. Anzolini, A. D. Mariani, *Opt. Express* **2013**, *21*, 11430.
- [15] P. Ghemini, P. Lomazzi, T. A. Gerner, J. W. Strapp, S. S. Vigna, M. G. Sotgiu, M. H. Jandori, J. C. Sanchez-Lopez, *J. Biomed Opt.* **2012**, *17*, 010114.
- [16] F. Tomita, E. Akita, C. Joseph, R. Giles, *J. Biomed Opt.* **2013**, *18*, 060504.
- [17] J. Magliński, C. MacKintosh, A. Kart, H. Voon, M. Eickel, *Biomedical Optics and 3D Imaging, 6th International Optical Society of America, DC, SPIE* **2012**.
- [18] R. Kuznetsov, C. MacKintosh, A. D'Amico, S. Jacques, M. Eickel, *J. Biomed Opt.* **2015**, *20*, 317.
- [19] V. Chibrikov, A. Gubarev, A. Spitsyn, A. Dubinin, O. Vashchuk, A. Ushakov, Y. Ushakov, M. Gostky, M. Sita, A. Rabin, *J. Magnets. Resonance* **2014**, *24*.
- [20] N. K. Ural, S. Chakraborty, R. Iyer, P. K. Dasgupta, I. Magliński, N. Ghosh, *Opt. Commun.* **2014**, *417*, 172.
- [21] M. Borekova, M. Pyrenich, Y. O. Ushakov, O. V. Dubinin, V. O. Ushakov, A. V. Ilyuk, T. P. Norkova, I. Magliński, *J. Exp. Opt.* **2014**, *43*, 20.
- [22] (a) D. Inoue, R. Oshikiri, T. Norkova, P. Li, B. Borekova, T. Goto, E. Nishikawa, D. Naito, *Proc. SPIE* **2019**, *11075*, 1107514. (b) D. Inoue, T. Goto, E. Nishikawa, I. Nishikawa, D. Naito, *Proc. SPIE* **2019**, *11047*, 1104707.
- [23] D. Inoue, E. Nishikawa, T. Goto, I. Nishikawa, D. Naito, *AP Opt. Phys.* **2019**, *20*, 170107.
- [24] M. Borekova, V. A. Ushakov, A. V. Dubinin, O. Ya. G. G. U. Vashchuk, A. V. Ilyuk, I. Magliński, *PLoS One* **2018**, *13*, e0210484.
- [25] A. Ushakov, A. A. Sobolev, M. G. Dubinin, V. Ushakov, A. Belyi, I. Magliński, *IEEE J. Sel. Top. Quantum Electron.* **2019**, *25*, 700012.
- [26] V. Drenina, D. Anis, O. Sisyi, M. Borekova, J. Nigamkang, I. Magliński, A. Belyi, *Proc. SPIE* **2020**, *11511*, 1151104.
- [27] D. Inoue, V. Drenina, A. Belyi, E. Nishikawa, T. Goto, A. Pappas, E. Oshikiri, T. Norkova, I. Magliński, *J. Biophotonics* **2020**, *11*, 20200002.
- [28] M. Borekova, A. Belyi, A. Pappas, A. Papatoglu, T. Norkova, A. Dubinin, I. Magliński, *Biomed Opt. Express* **2020**, *11*, 4008.
- [29] N. Nishikawa, K. Nishiyoshi, H. Mankata, *Proc. Natl. Acad. Sci. U S A* **2017**, *114*, 1181.
- [30] N. Nishikawa, M. Araya, R. C. Eiza, E. Nishiyoshi, H. Mankata, *Appl. Phys. Exp.* **2018**, *11*, 050501.
- [31] R. C. Eiza, N. Nishikawa, K. Nishiyoshi, H. Mankata, *J. Appl. Phys.* **2018**, *123*, 233901.
- [32] R. C. Eiza, N. Nishikawa, H. Mankata, *SPIN* **2018**, *08*, 2100077.
- [33] N. Nishikawa, A. Tamaki, K. Takahashi, T. Kuchimaru, H. Mankata, *Opt. J. Appl. Phys.* **2020**, *20*, 381003.
- [34] N. Nishikawa, S. Kawahira, H. O. Qadi, T. Kuchimaru, H. Mankata, *Proc. SPIE* **2020**, *11571*, 1157114.

SUPPORTING INFORMATION
Additional supporting information may be found online in the Supporting Information section at the end of this article.

How to cite this article: Nishizawa N, Ali Qadi B, Kuchimaru T. Angular optimization for cancer identification with circularly polarized light. *J. Biophotonics*. 2020;e202000380. <https://doi.org/10.1002/jbip.202000380>

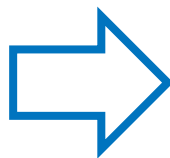
論文の探し方

論文検索サイト

- Google Scholar ← 私のオススメ
- Web of Science
- PubMed

英語で検索すること
 専門用語で検索すること
 △ stomach cancer
 ○ gastric cancer

ある特定の情報が得たい場合、
 自分の研究に用いるデータを探す場合、
 自分の研究に似た研究を探す場合、



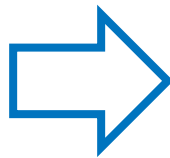
キーワードをできれば複数
 動詞を入れる、出版年代を限定する
 限定検索にするなどで絞れることがある
 また、検索結果をサイト検索でスクリー
 ニングするのも手である

ある論文を基にその論文の周辺論文を
 調べる場合、
 特定の手法や現象の原理を知りたい場
 合、



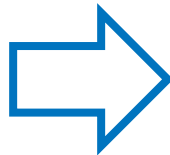
その論文の引用文献から探る方が早い
 引用文献は代表となる論文を挙げてい
 るので選択しなくても重要であることが
 わかる

ある論文のその後を発展やどう使われた
 かを知りたい場合



その論文のページにある“cited by”を調
 べる(その論文を引用した論文のリスト)

研究全体の流れや歴史を捉えたい



Review論文を探す“Reviewed paper”で
 検索(ただし長編であることが多い)

Top 5 Free Tools for an Effective Literature Search

ARXIV DISCOVERY

- 250M+ Research Papers (incl. 40M+ OA articles)
- Personalized Reading Feed with New Paper Alerts
- Multilingual & Full-Text Audio
- Integration with Zotero/Mendeley
- Gen AI Search, Summarized Answers With References

GOOGLE SCHOLAR

- Largest Repository with 350M+ Papers
- Export Citations in Various Formats
- Monitor Citations and Research Ranking
- Create a Public Author Profile
- Locate the Complete Document

PUBMED

- 37M+ Research Papers
- Top Source for Biomedical and Life Sciences Literature
- MeSH Terms Added for Better Search Results
- Save, Email, or Export citations in Various Formats

SEMANTIC SCHOLAR

- 220M+ Academic Papers
- Quick Paper Assessment
- Save, Annotate, and Track Metrics (Citations, h-index)
- Enhanced PDF Reader with Definitions, Citations, and More

LENS

- 200M+ Scholarly Records
- Largest Public Patent Database
- Create, Annotate, and Personalize Patents and Scholarly Works
- Explore Scholarly Influence on Patents and Products